technologies

MDPI

Article

"The Foot Can Do It": Controlling the "Persistence" Prosthetic Arm Using the "Infinity-2" Foot Controller

Peter L. Bishay *, Gerbert Funes Alfaro, Ian Sherrill, Isaiah Reoyo, Elihu McMahon, Camron Carter, Cristian Valdez, Naweeth M. Riyaz, Sara Ali, Adrian Lima, Abel Nieto and Jared Tirone

Department of Mechanical Engineering, California State University, Northridge, CA 91330, USA
* Correspondence: peter.bishay@csun.edu

Abstract: The "Infinity" foot controller for controlling prosthetic arms has been improved in this paper in several ways, including a foot sleeve that enables barefoot use, an improved sensor-controller unit design, and a more intuitive control scheme that allows gradual control of finger actuation. Furthermore, the "Persistence Arm", a novel transradial prosthetic arm prototype, is introduced. This below-the-elbow arm has a direct-drive wrist actuation system, a thumb design with two degrees of freedom, and carbon fiber tendons for actuating the four forefingers. The manufactured prototype arm and foot controller underwent various tests to verify their efficacy. Wireless transmission speed tests showed that the maximum time delay is less than 165 ms, giving almost instantaneous response from the arm to any user's foot control signal. Gripping tests quantified the grip and pulling forces of the arm prototype as 2.8 and 12.7 kg, respectively. The arm successfully gripped various household items of different shapes, weights, and sizes. These results highlight the potential of foot control as an alternative prosthetic arm control method and the possibility of new 3D-printed prosthetic arm designs to replace costly prostheses in the market, which could potentially reduce the high rejection rates of upper limb prostheses.

Keywords: foot control; wrist actuation; robotic arm; 3D-printing

Academic Editors: George F. Fragulis and Daniele Giansanti

Received: 23 December 2024
Revised: 18 February 2025
Accepted: 21 February 2025
Published: 1 March 2025

Citation: Bishay, P.L.; Funes Alfaro, G.; Sherrill, I.; Reoyo, I.; McMahon, E.; Carter, C.; Valdez, C.; Riyaz, N.M.; Ali, S.; Lima, A.; et al. "The Foot Can Do It": Controlling the "Persistence" Prosthetic Arm Using the "Infinity-2" Foot Controller. *Technologies* **2025**, *13*, 98. https://doi.org/10.3390/technologies13030098

1. Introduction

A recent study was conducted by Salminger et al. [1] in 2020 to assess if new innovations and refinements in prosthetic technology had an impact on the previously reported high upper limb prostheses rejection rates, reported in [2]. Surprisingly, it was found that the advancements of upper limb prosthetics in the last decade had not yet achieved a significant change in prosthetic abandonment. The rejection rate was 44% among 68 individuals with traumatic upper limb loss in Austria. The three major concerns shared by the participants were comfort, device weight, and functionality. Among users, 93% used myoelectric controllers, which reflects the dominance of this control method in controlling powered prosthetic arms. Although academic solutions were proposed to address the patient's complaints, clinical reality has not fully benefited yet from the new advances to cause any improvements in prostheses acceptance rates.

Myoelectric control systems use electromyographic (EMG) signals from residual muscles to control the prosthetic device. Myoelectric controllers have moved from the early single-site EMG sensors to pattern-recognition systems that rely on machine learning to interpret multiple muscle signals [3]. Although this enabled control of multi-degree-of-freedom prostheses, the limitations of this control approach still exist. Myoelectric control systems are affected by the skin condition and cause muscle fatigue. The number of unique

control commands is still limited. If the amputation resulted in the absence of muscle function in the residual limb, EMG control would not be an option. This happened with the individual who was not even fitted with a prosthetic arm in the aforementioned recent study [1] due to the absence of muscles in the residual limb. EMG systems are also unreliable and unpredictable according to a recent study by Chadwell et al. [4] that revealed that EMG prostheses users tend to produce undesired activations of the hand or incorrect responses. Franzke's study [5] also proved the dissatisfaction of myoelectric users with the process of switching prosthesis function under conventional control. Pattern recognition was appreciated as an intuitive control that facilitated fast switching between prosthesis functions but was reported to be too unreliable for daily use and require extensive training.

In the state-of-the art review of prosthetic arm systems conducted by Vujaklija et al. [6] in 2016, it was concluded that the current bottleneck of the upper limb prosthetic development seems to be the control of the robotic limbs. Various other non-invasive control approaches were proposed, such as electroencephalography (EEG) [7–9], voice control [9–13], and foot control [14–20]. EEG requires placing multiple brain wave sensors on the head, usually in a headset to be worn by the prosthetic arm user, which is considered a limitation on its own. It also requires significant training and mental concentration during use and is affected by the placement and amount of hair on the head [21]. The reliability level is also lower than other control methods [9]. Despite the current advances in voice recognition technologies, using voice control for prosthetic arms requires the user to talk to the device to control the arm, which would not be desirable in all situations. Noise could affect the reliability of the system [21], and security measures would be needed to prevent others from controlling the user's arm.

Alderson [22] was the first to propose a foot controller for above-the-elbow individuals with upper limb loss of "extreme cases", who have extremely short stump, no stump at all, or a stump of moderate length but with impaired muscular function. The controller included toe contacts in a sole to be worn inside the user's shoe. His patent, that focused mainly on the design of a prosthetic arm, was filed on 10 July 1948, and was granted on 1 January 1952. In 1968, Alderson wrote a chapter on an improved version of his invention in the "Human Limbs and Their Substitutes" book [23]. To resolve the problem of accidental operation of toe controls during walking, he assigned only the little toe to control the motor of the hand, while the big toe and heel were used to select the functions of the motor. This was based on a peculiarity of toe actions he found that the little toe exerts only light pressures in a normal gait but could be pressed down with considerable force when desired. To operate the arm, the little toe should be pressed first followed by the big toe or heel. Control signals from the foot were directed to the arm mechanisms by means of pneumatic bladders embedded in a plastic insole and connected by thin rubber tubing to corresponding bladders in the arm. In 1974, Graupe [24] eliminated the need for three toe movements that were required per limb function in Alderson's invention, and used microelectronic hardware (strain gages) that were unavailable in 1952 to enable control of the prosthetic hand using one toe movement in his proposed controller idea. His system was operational only during sitting, lying, or standing, but was inhibited during walking. Using the natural anatomic and physiologic similarities between the upper and lower extremities, which makes the foot and leg to be an ideal control interface, Luzzio [25], in 2020, developed a stocking laced with multiple sensors to provide input on multiple leg joint positions. The signals were used to control homologous movements in a prosthetic upper extremity. The significant advantage of this form of control, compared to earlier inventions, was the simultaneous activation of multiple joints. Carrozza et al. [26,27] developed a prototype of a wearable insole, called ACHILLE insole, with FSR switches placed at four sensitive areas (heel, big toe, lateral left, and lateral right). The prototype

used wireless transmission to control a robotic hand prosthesis with three fingers. Testing it on 10 able-bodied subjects showed a significant decrease in required adaptation and learning from the user's side, compared to EMG control.

Lyons and Joshi [16] conducted an important study in 2015 where EMG sensors were placed on the forearm to record the muscle activity while participants performed gestures with their dominant hand. Then, the sensors were placed on the lower leg while participants performed analogues set of foot gestures. An intuitive mapping between the hand and foot was found and determined to be sufficient for prosthetic control. Accordingly, they used surface EMG (sEMG) sensors placed on the lower leg and mapped the degrees of freedom of the leg to those of the arm to enable noninvasive control of prosthetic elbow, wrist, and hand movements [17,18]. Lee et al. [20] used a wearable fabric sensor on the lower leg to map foot postures to prosthetic hand postures. Their experimental results confirmed that the sEMG signals of the lower limb obtained by using their developed sensors were more distinct than those of the upper limb for eight postures. DEKA Research [28] developed a prosthetic arm along with a foot controller [29] that includes force sensitive resistors (FSRs) in a custom made insole along with inertial measurement units (IMUs). Resnik et al. [19] tested the DEKA foot controller [30] on 36 subjects with upper limb amputation, 77% of whom owned a myoelectric device, 22% owned body-powered devices, and 14% owned a cosmetic arm or no prosthetic device at all. Although some of the subjects described the used FSR or IMU controllers on both feet as "bulky", the subjects' feedback was generally positive. The "Infinity" foot controller developed by Bishay et al. [15] used two push buttons in an insole under the toes to control the fingers of the prosthetic arm, along with a sensor controller unit (SCU) to actuate a two-degree-of-freedom wrist actuation system in the arm. This system relied on the big toe and four lesser toes to control the prosthetic arm fingers in multiple grips, which was shown to be an easy and intuitive control method.

Commercial prostheses are often unaffordable, or inaccessible, to underprivileged individuals (e.g., no health insurance, low incomes, warzone). In addition, each design of a commercial arm has its own limitation. For example, the Hero Arm [31], which is a lightweight, below-the-elbow prosthesis, lacks wrist flexion/extension and pronation/supination movements. Commercial prostheses are also limited in terms of customizability, as they come in standard sizes, and with specific control systems. Some prostheses also require inputs from a natural hand to adjust the orientation of the wrist manually. Piazza et al. [32] presented a state-of-the-art review of artificial hands covering 106 years of engineering (1912–2018). The review included some famous commercial prosthetic arms, such as the Ottobock Michelangelo Hand [33], the i-Limb Quantum [34], the Open Bionics Hero Arm [31], and the BeBionic hand [35]. They concluded that using new fabrication technologies is opening the way to a reduced cost of production of artificial hands. Wendo et al. [36] in 2022 presented a review on open-source 3D-printed upper limb prostheses, as this new fabrication technology offers higher availability and accessibility and can produce complex geometrical and highly customized products, which are essential features for prostheses manufacturing. However, more work is needed to expedite the implementation of 3D-printed prostheses in clinical routines and their acceptance by the healthcare providers community.

In this paper, a modified version of the Infinity foot controller that was originally proposed in [15] is presented. The new features of this controller, named "Infinity-2", include a foot controller sleeve (FCS) that replaces the foot controller insole to enable a more secured fit around the foot when the user is using the controller shoeless. In addition, Bluetooth and Wi-Fi technologies are used in wireless data transmission, leading to high response speeds from the prosthetic arm when the user makes an action with the foot controller. Gradual control of finger deformation has also been achieved through a new

control scheme. To demonstrate the capabilities of the foot controller, a new transradial prosthetic arm prototype, named the "Persistence" arm, has been designed. Compared to the Infinity arm reported in [15], this new arm includes a powerful direct drive wrist actuation mechanism, a lightweight forearm core structure with generatively designed mounts, a separate forearm outer shell, four three-digit forefingers that are actuated with carbon-fiber ribbons connected to individual servomotors housed in the palm structure, and a two-degree-of-freedom linkage-based thumb. The whole system has been tested in various tests to prove that the design goals have been successfully achieved. The goal of the whole proposed system is to give the user a simple, effective, reliable, and comfortable way to control their below-the-elbow prosthetic arm utilizing the human's natural connection between the arms and feet.

The rest of the paper is organized as follows: The next section, Materials and Methods, describes all features of the Infinity-2 foot controller, Persistence arm, and the manufacturing and assembly of both. The Results section comes next with details on the performed actuation and gripping tests. This is followed by a Discussion section, and then the paper is concluded in the Conclusions section.

2. Materials and Methods

2.1. Infinity-2 Foot Controller Design

The Infinity-2 foot controller system is shown in Figure 1. It is a two-part system that includes the Foot Controller Unit (FCU) and the Foot Controller Sleeve (FCS).

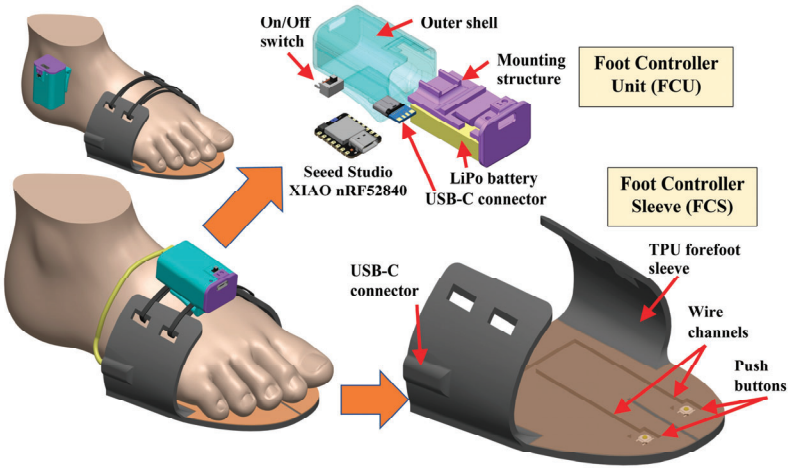

Figure 1. Infinity-2 foot controller system.

The FCU and FCS work together to control a below-the-elbow prosthetic arm that has up to five fingers and two wrist degrees of freedom (DOF), namely wrist flexion/extension and pronation/supination. The FCU contains a Seeeduino XIAO BLE nRF52840 Sense microcontroller (Manufacturer: seeed studio, Shenzhen, China), a rechargeable 400 mAh LiPo battery, an on/off switch, and a USB 3.1 Type C female connector. All these electronic components are secured on the main mounting structure and covered by the outer shell, as shown in Figure 1. The mounting structure and the outer shell are both made of 3D-printed Polylactic Acid (PLA) material. The outer shell has an integrated clip to facilitate attaching the FCU to the FCS, to the collar of a shoe, or to the cuff of a sock. The Seeeduino microcontroller does not only have the 6 DOF Internal Measurement Unit (IMU), which encases an accelerometer and a gyroscope, but it also has a Bluetooth antenna, a battery charger, and a very fast processor to process the IMU data. With an embedded LED, this microcontroller also lets the user know the charge level of the battery. The microcontroller

processes all gyroscopic and accelerometer data, which is then sent to the prosthesis and is used to actuate the wrist servomotors. The gyroscope measures the current position of the user's foot. When rotating the foot around the pitch axis (ankle dorsiflexion and plantarflexion), the user can control the wrist extension and flexion, and when rotating the foot around the roll axis (ankle inversion and eversion), the user can control the wrist supination and pronation, as illustrated in Table 1. This allows the user to place their prosthetic palm in multiple different positions for a better grip of objects with various shapes and sizes. Rotation around the yaw axis (ankle abduction and adduction) is negated, as it is used to re-center the device when walking detection is activated.

Table 1. Foot motions and resulting hand motions.

Foot motion	Ankle dorsiflexion	Ankle plantarflexion	Ankle inversion	Ankle eversion	Big toe press	Lesser toes press	All toe press
							
	Wrist extension	Wrist flexion	Wrist supination	Wrist pronation	Fingers flexion	Fingers extension	Grip change
Resulting hand motion		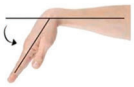					

The FCS allows the user to gain finger actuation control as finger flexion and extension in various grip patterns. The FCS consists of four layers, as shown in the exploded view in Figure 2. The forefoot sleeve layer houses all electronics and is 3D-printed of Thermoplastic Polyurethane (TPU), which is a flexible material, to allow the sleeve to deform around the forefoot. This gives a custom fit for the FCS around the user's foot, whether on a barefoot or a sock, or inside a shoe. The sleeve layer is supported by a three-part support layer underneath, which is 3D-printed of Acrylonitrile Butadiene Styrene (ABS) and has channels for push buttons and wires. The button paddles layer is placed above the sleeve layer to increase the surface area of the clickable regions under the tows that can push the buttons placed under them.

This design distributes pressure across the button and its surrounding area, making it easier to press successfully, even if the toes are not perfectly aligned with the button position. The paddles layer is 3D-printed of TPU material. The top layer is made of felt to give comfort to the user. The two push buttons are connected to the USB-C connector through wires routed in the channels. An external USB-C cable is used to connect the FCS to the FCU, as shown in Figure 1. The wiring diagram of the FCU and FCS is shown in Figure A1 in Appendix A.

Each prosthetic arm and FCU have their own set of Universally Unique Identifiers (UUIDs) that are used to pair the devices together. When the FCU is powered on, the device follows the control flowchart shown in Figure 3. First it starts setting up its internal Bluetooth UUID's. Soon after, it enables Bluetooth discoverability. The device then waits for a connection to be established. If the FCU manages to connect to a device, it then closes Bluetooth discoverability, checks its battery level, then moves into a standby mode until an action is done. If the IMU is triggered by motion, the gyroscope then calibrates itself

to correctly assign its axes using the yaw axis as the neutral axis. It then checks if the user is walking. If no walking is detected, the action that was done is then transmitted to the prosthetic arm as a corresponding axis value. After checking the battery level, the FCU also processes the button data that comes from the FCS. It checks if the buttons are being pressed or held. If no button has been pressed, it keeps waiting for a button press. If a button is pressed, the FCU goes to the walking detection check, followed by the data transmission step to the prosthetic arm's MAC address.

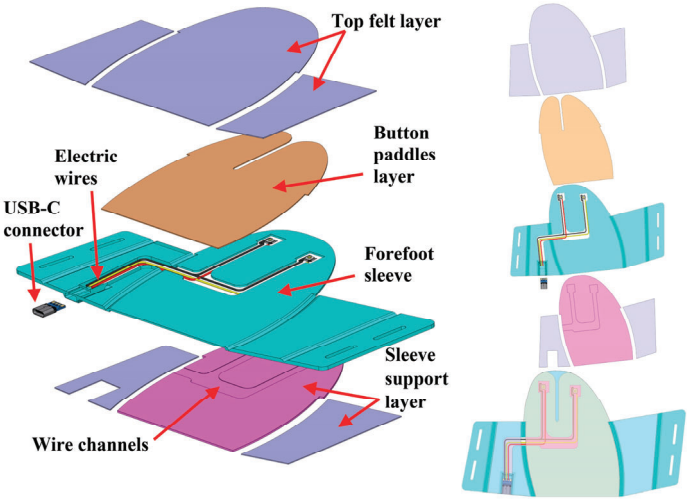

Figure 2. Foot controller sleeve (FCS) in exploded view.

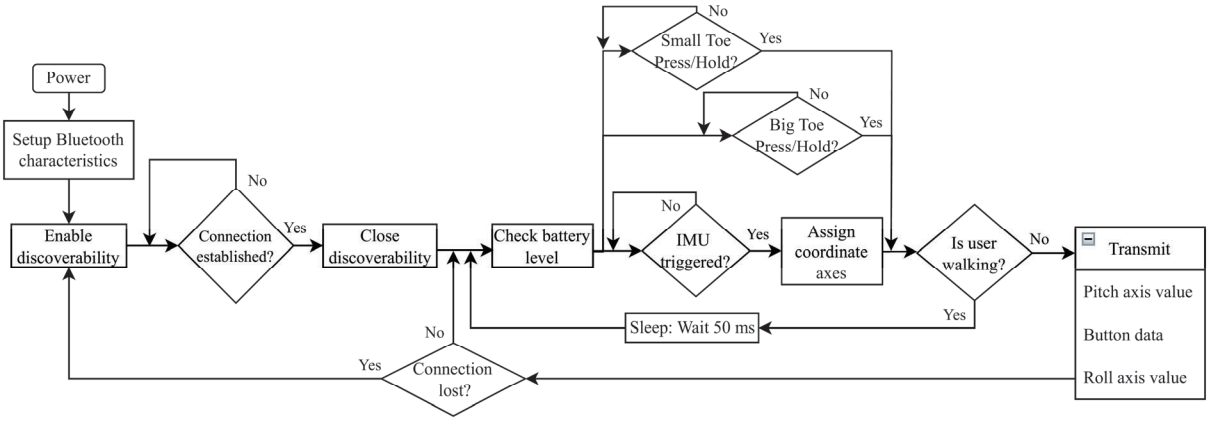

Figure 3. FCU control flowchart.

To determine if the user is walking, the FCU goes through the process shown in Figure 4. This process is done before any data is determined to be ready for transmission. Once the IMU trigger has been determined, the IMU checks all gyroscope axes along with all accelerometer values for all axes. If any two axes are both above their specified threshold for both the gyroscope and accelerometer values, the user is determined to be walking with the device. The threshold values can be adjusted for each user. Testing determined the default values to be used for most users. The threshold was intentionally set to be more sensitive, increasing the likelihood of false-positive walking detections rather than missing actual walking. As a result, the FCU may occasionally classify the user as walking if they rotate their ankle rapidly while attempting to control the wrist. The obtained threshold values allowed different users to utilize the device and confidently walk without worrying about the prosthetic arm actuating while walking.

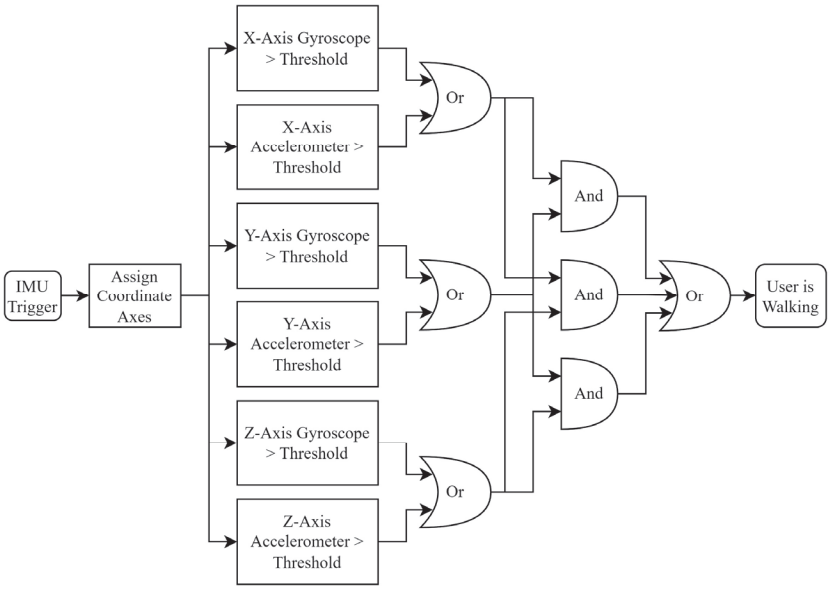

Figure 4. Walking detection system flowchart.

2.2. Persistence Arm

Figure 5 shows the full CAD assembly of the Persistence Arm. The palm contains five lightweight digital servos that actuate the five fingers. The thumb has an additional servomotor to add a second degree of freedom to the thumb actuation. The forearm contains the wrist actuation mechanism as well as the electronics responsible for controlling and supplying power to the arm. The wrist actuation system occupies 50% of the forearm length.

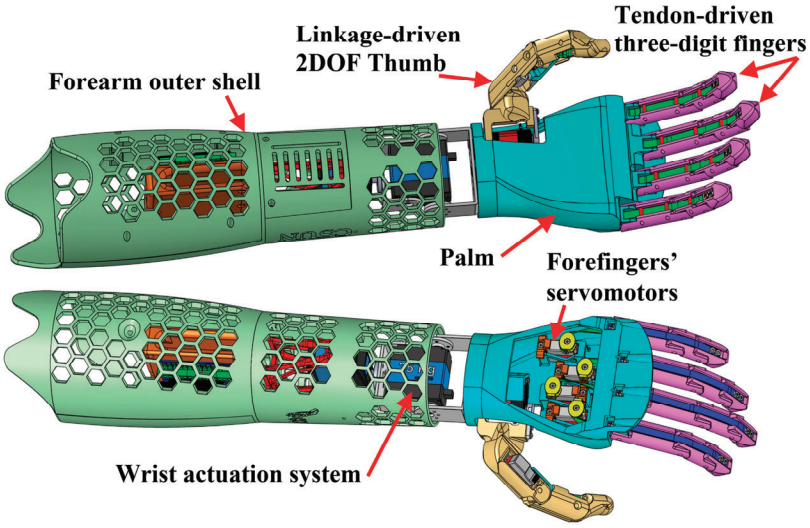

Figure 5. Full CAD assembly of Persistence arm.

The palm was designed to be as biomimetic as possible, taking inspiration from the human hand. The shape, size, and proportions of the Persistence palm were made to resemble an average-sized male hand. However, since the whole CAD model was created parametrically, the size can be reduced to the average female hand size with some adjustments, including reducing the number of forefinger servomotors from 4 to 3, coupling the actuation of the ring and pinky fingers, since they move together in all programmed grips. A similar coupling was done in [15]. The resizing of the CAD model would not

affect the components that have standard sizes, such as the servomotors, and locations and dimensions of mounting points. The assembly and exploded views of the palm with its fingers can be seen in Figure 6. The palm has attachment points for each of the fingers. The index, middle, ring, and pinky fingers are secured to the palm using M3 screws that are threaded into heat-set inserts located in the palm. The thumb is attached to a dedicated mount inside the palm, which has its own set of heat-set inserts and a rotating pin at the bottom.

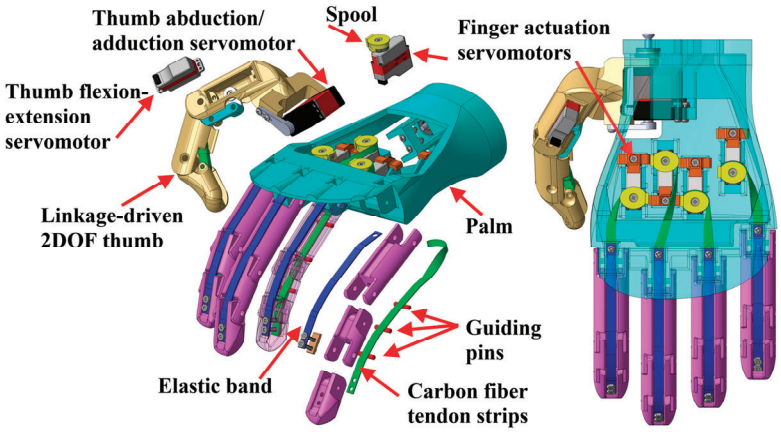

Figure 6. Persistence hand in exploded and assembled views.

The four forefingers are actuated using four KST A08N micro servomotors (stall torque: 3.2 kg.cm at 8.4 V; max. speed: 0.09 s/60°; weight: 7 g; size: 23.5 × 8 × 19 mm). Each servomotor has a spool connected to its shaft. As shown in Figure 7a, a flexible carbon fiber tendon strip, from Carbitex (www.carbitex.com), is attached to each spool and is routed through a special groove in the three finger phalanges. It is then attached to the distal phalange with two retaining screws. When the servomotor operates, it turns its spool, transferring the servomotor's torque into a pulling force on the tendon strip to flex the finger. All three phalanges of the finger move at the same time to close the finger. However, the finger can take different shapes depending on the contour of the object it touches. This compliant behavior enables the hand to grip objects of different shapes and sizes since each finger can deform independently and surround the object in the closest possible way. If the finger does not face any obstacles or objects to grip, it will close on itself. Hence, this design allows for different grips and gestures to be realized by the prosthetic hand, mimicking the human hand's natural deformations.

The spool on the servomotor has a radius of 7 mm, which is big enough to pull the carbon fiber strip just the right amount to fully close the finger. This is done with about 160° rotational movement of the spool by the servomotor. The phalanges of the finger are attached to one another using screws connected to heat-set inserts embedded in the phalanges. Guiding pins are assembled to the phalanges, as shown in Figure 7a, to guide the carbon fiber tendon strip as it slides in its groove when finger flexion happens and to reduce friction. Finger extension is achieved by the elastic band attached and routed through the top side of the finger to allow the finger to fully return to a relaxed position when the servomotor is set to an idle condition. The elastic bands have special channels embedded in the phalanges that allow each band to conform around the finger when it is actuated.

The Persistence arm's thumb has a linkage-based design, different from the design of the forefingers. This design, shown in Figure 7b, enables the thumb to have two degrees of freedom: flexion/extension and abduction/adduction. The flexion/extension servomotor

is a KST A08N housed inside the proximal phalange to actuate the middle and distal phalanges via the linkage mechanism. The base of the proximal phalange is connected to the palm, as shown in Figure 8. The base houses the abduction/adduction KST A12-610 servomotor (stall torque: 9 kg.cm at 8.4 V; max. speed: 0.10 s/60°; weight: 20 g; size: 23 × 12 × 27 mm). The thumb base sits on a bearing and a pin inserted in a slot in the palm structure at the location of the metacarpal. This enables the abduction/adduction servomotor to rotate the thumb without friction up to 70°.

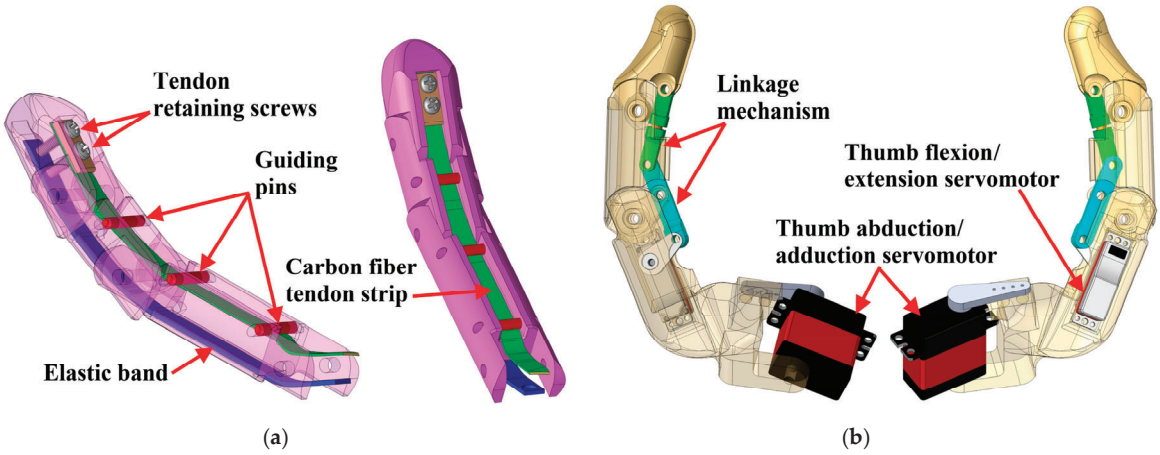

Figure 7. Persistence arm fingers: (**a**) a forefinger, and (**b**) the thumb.

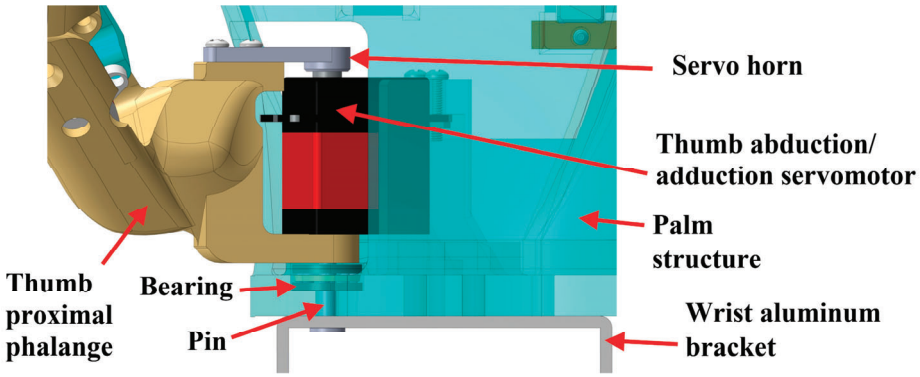

Figure 8. Thumb's connection to the palm structure.

Persistence arm features two wrist degrees of freedom: wrist flexion/extension and wrist pronation/supination. The assembly of the wrist actuation mechanism inside the forearm is shown in Figure 9, with a transparent outer shell to show the internal components. The design features a wrist mount that houses the wrist pronation/supination servomotor, which is a 35 kg DS3235 servomotor (stall torque: 35 kg.cm at 7.4 V; max. speed: 0.11 s/60°; weight: 60 g; size: 40 × 20 × 38.5 mm). An aluminum bracket connects this servomotor to the wrist flexion/extension servomotor, which is a dual bearing 35 kg RDS3235 servomotor (stall torque: 35 kg.cm at 8.4 V; max. speed: 0.11 s/60°; weight: 60 g; size: 40 × 20 × 40 mm). Another aluminum bracket connects this servomotor to the palm structure. This pant-tilt system allows the wrist to rotate 90° in both directions for a 180° range of pronation/supination and to tilt 30° degrees in both directions for a 60° range of wrist flexion/extension.

The control system in the arm includes an ESP-WROOM-32 microcontroller (Manufacturer: Espressif Systems, Shanghai, China), which receives all signals from the foot

controller and actuates all servomotors in the arm. A 7.4 V LiPo battery powers all servomotors in the arm through a terminal block. The wiring diagram of the arm is shown in Figure A2 in Appendix A.

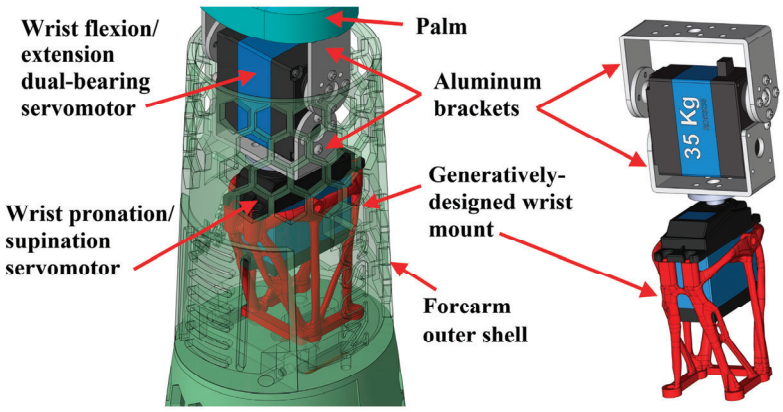

Figure 9. Wrist actuation mechanism in Persistence arm assembled inside the forearm with transparent outer shell.

The Generative Design (GD) tool in Autodesk Fusion was used to design the wrist mount shown in Figure 9. Based on defined preserve regions, obstacle regions, load conditions, material parameters, and manufacturing methods, this tool runs a machine learning (ML) algorithm to iteratively optimize the design. The GD algorithm follows a process of generation, evaluation, and evolution, to optimize the design by reducing mass and maximizing stiffness while still satisfying all defined initial conditions. Appendix B gives more details on the process of creating this mount using the GD tool.

The electronics of the control system are all mounted on a 3D-printed PLA mount in the upper part of the forearm, as shown in Figure 10. ESP-32 is mounted on one side, and the terminal block is mounted on the other. The LiPo battery is placed beside the terminal block. The outer shell of the arm, shown in Figure 5, Figure 9, and Figure 10, is perforated to reduce weight and is made of two parts: the lower part, which surrounds the wrist actuation mechanism, and the upper part, which surrounds the electronics mount. Both parts are connected using four M3 screws that are also securing the wrist mount to the shell. Three M2 alignment screws are also used to strengthen the connection of the upper and lower parts of the forearm shell. Two access points are included in the outer shell. The first is a small door in the lower part, as shown in Figures 5 and 9, and the second is a bigger door in the upper part. The doors are connected to the main body of the shell using M2 screws. The shell is connected to the socket on the residual limb.

Figure 11 shows the Persistence arm's control flowchart. When the arm is powered on, the device checks all motor positions. If any motor is not in its default position, the arm adjusts and resets the motor to bring it back to its default position. Default positions for this arm are as shown in Figure 5: All fingers are fully open, and the wrist is straight with the palm. At the same time, the arm is searching for its designated Foot Controller Unit (FCU) to be paired with via UUID. As a safety measure, a second unique identifier is also used in the pairing procedure to ensure the correct device has been connected. The two devices need to match a password in order to establish a full connection. There is one additional level of security that is built into the transmission. The payload messages have a unique structure that is known to the arm. If the message does not match the structure the arm is expecting, the arm will reject the message. Figure 12 shows the flowchart of the security checks.

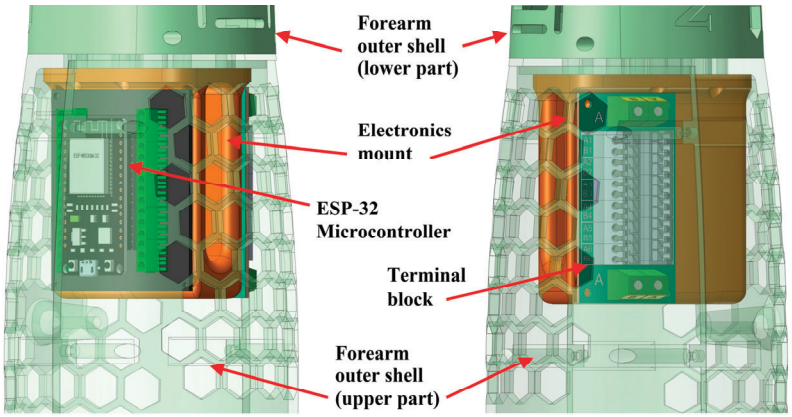

Figure 10. Electronics mount in the upper part of the forearm with transparent outer shell (two sides).

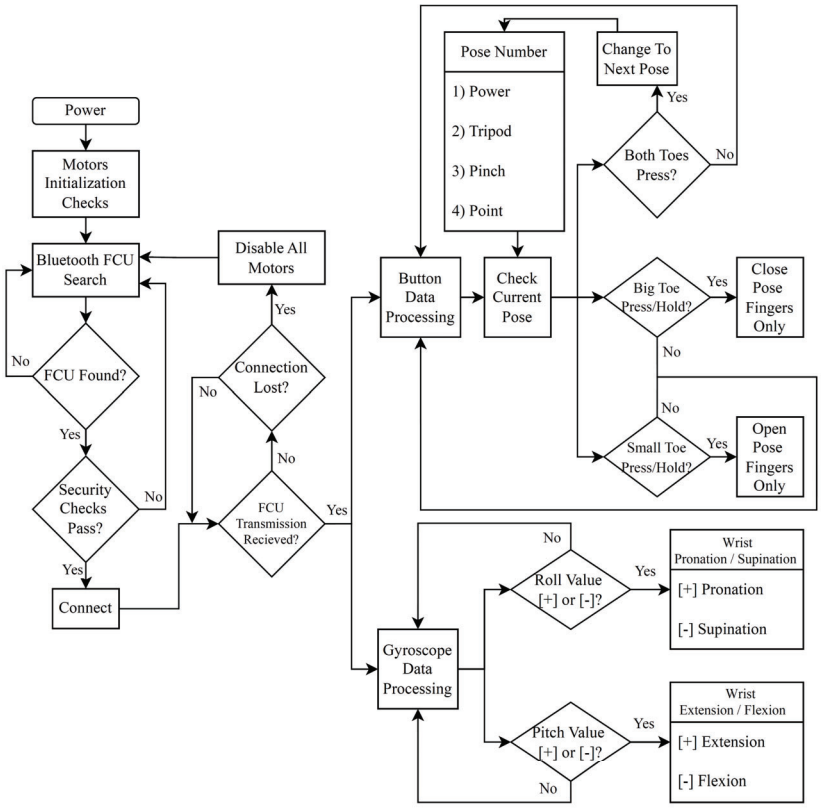

Figure 11. Persistence arm control flowchart.

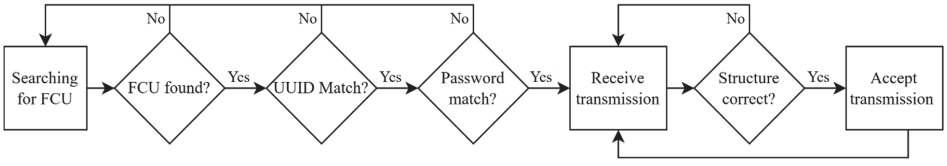

Figure 12. Security checks used in wireless communication between Persistence arm and Infinity-2 foot controller.

After all security checks have passed and the FCU has established a connection, the arm can work as intended. When the raw gyroscope data is received from the FCU, the arm processes this data and translates the received values to their corresponding movements.

Both the roll and pitch values can be positive or negative. If the pitch value is positive, the wrist extends; if it is negative, the wrist flexes. For pronation/supination, if the roll value is positive, the wrist supinates; if it is negative, the wrist pronates. Both wrist flexion/extension and wrist pronation/supination move at a speed of 2° per transmission. Preliminary testing showed that this rate gives the user a good middle ground between speed and precision and allows the user to gradually orient the prosthetic palm in the user's desired position.

Processed button data is sent by the FCU to the arm. When this data is received, the arm performs a check before moving any fingers to find out what pose it is currently going to do. The default starting pose is the "Power" pose. The user can cycle between the four assigned poses by pressing both toe buttons simultaneously. The poses will cycle in the following order: power, tripod, pinch, point. When the pose is identified, the arm moves the appropriate fingers required by that specific pose. If the user presses the big toe button, the arm gradually flexes the desired fingers by 5° for the four forefingers. The thumb metacarpal will adduct by 1°, while the thumb phalanges will flex by 2°. If the user presses the lesser toes button, all fingers extend, and the thumb abducts by the same rate used in closing. This happens once for every single transmission received, allowing the user to hold any of the two buttons down and move the fingers gradually, or get precise movement by simply pressing any of the buttons to move the fingers by just one step to adjust the grip strength to the desired amount. The arm remembers the exact position of each specific finger even if the user switches to a different pose. When the fingers are actuated, all servomotors involved in the selected pose will move gradually as long as the big toe button is pressed. Once the button is released, the fingers stop immediately. If the user changes the pose at this point and then presses the button again, only the servomotors for the newly activated fingers will move, while the others remain in their last known positions until reactivated. If the user then chooses to open the fingers from this new position, all fingers will gradually open together, regardless of the pose. An example of this would be as follows. The user begins with the Power grip, where all five fingers are to be actuated. The fingers gradually close until they reach approximately 35% of their full actuation range. At this point, the user realizes that the object can only be grasped using the tripod grip, which involves the thumb, index, and middle fingers only. They switch to this pose and continue closing these three fingers until they reach around 75%. Meanwhile, the ring and pinky fingers remain at their last known position of 35%. When it is time to release the object, all fingers, regardless of whether the pose is power or tripod, or whether their position was at 35% or 75% of their actuation range, will gradually open until fully extended. If the user starts with a pinch grip (only thumb and index) and then after 40% actuation, switch to power grip, all fingers will move with the same rate until they touch an object or reach their full actuation range. However, in this case, the middle, ring, and pinky fingers will start actuation from their fully extended position, whereas the thumb and index would resume from their 40% actuated positions. Persistence arm can handle parallel processing of the systems discussed: wrist flexion/extension, wrist pronation/supination, and finger gripping. This means that if the user would like to close the fingers while also rotating the wrist, the prosthesis will be able to process both commands and actuate the corresponding servomotors simultaneously.

2.3. Manufacturing and Assembly

All structural components, such as finger phalanges, forearm outer shell, and forearm electronics and wrist mounts, were first 3D-printed of PLA, then electronic components were assembled. Only the palm was 3D-printed of ABS to prevent any possible overheating of the forefingers' servomotors from deforming their mounts in the palm structure, since

ABS performs better in heat resistance scenarios than PLA (the glass transition temperatures of ABS and PLA are 105 °C and 60 °C, respectively). Figure 13 shows the fully assembled proof-of-concept model of the Persistence Arm. Each finger servomotor was secured in its housing inside the 3D-printed palm via a system of heat inserts and screws. Heat inserts were also embedded in all finger phalanges, and then screws were connected to act as joints. 2 mm dia. brass pins were also secured in the fingers to act as guides for the carbon fiber tendons that slide in the finger bottom channels during finger actuation. The flexible Carbitex carbon fiber tendon sheet was cut into strips, and the strips were routed through the fingers to the palm. Within the palm, they were attached to the spools of the servomotors using clamps and screws. The elastic bands were also routed through the top channel of the four forefingers to return the fingers to the neutral position when the fingers are not actuated. The internal links of the thumb were first assembled separately and connected to the flexion/extension servomotor. The thumb with its adduction/abduction mount was then attached to the palm using a thrust ball bearing held in position using a guide screw. Strips of rubber tape were bonded to the fingertips and palmer side of the palm to give the hand additional grip friction.

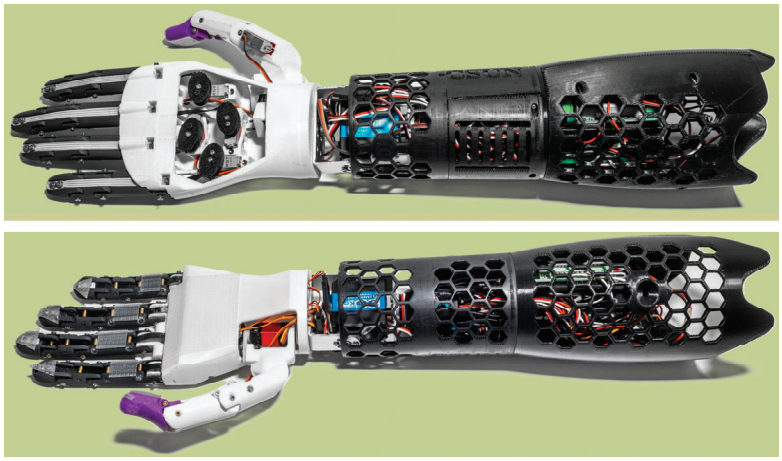

Figure 13. Assembled proof-of-concept model of the Persistence arm.

The wrist actuation servomotors were also assembled and mounted to the generatively designed wrist mount, as shown in Figure 14. The wrist mount and all other electronic components were secured on the forearm core structure and covered with the forearm outer shell. The assembled hand was then connected to the assembled forearm. The total weight of Persistence Arm without a battery is 670 g. The arm with a battery installed weighs 820 g.

The FCS forefoot sleeve and button paddles layers were 3D-printed of TPU material. The three-part support layer was 3D-printed of ABS to provide structural rigidity, and the top felt layer was cut to size. The push buttons were placed snugly in their specified pockets in the forefoot sleeve, and wires were routed through their guide channels and connected to the USB-C connector. All layers were then bonded together using Loctite superglue. The top felt layer gives the user a comfortable, soft feel when they put on the device. Figure 15a shows the assembled foot controller system. A Velcro strap was used to tighten the sleeve around the user's foot securely. The manufactured FCS weighs 31.2 g.

The FCU's outer shell and mounting structure were 3D-printed of PLA. All electrical components were then secured on the mounting structure. Then the outer shell was placed to cover and protect all components, as shown in Figure 15b. The outer shell's integrated clip is used to attach the FCU to the FCS, as shown in Figure 15a, or to the user's shoe

collar or sock cuff. The manufactured FCU weighs 51 g. The whole foot controller system, including the short USB-C cable, weighs 96.4 g.

The manufacturing cost of Persistence Arm was $390 and that of the Infinity-2 foot controller was $80. This does not include service charges for 3D-printing, and labor cost for manufacturing and assembly.

Figure 14. Manufactured wrist actuation mechanism.

(**a**) (**b**)

Figure 15. (**a**) Assembled foot controller system, (**b**) Foot controller unit (FCU).

2.4. Test Setup

To determine the wireless transmission speed between the foot controller to the arm's ESP32 microcontroller, the devices were connected to a computer via USB connection to log transmission times between both devices using a developed MATLAB code (version R2024a). The goal of the code was to record the time it takes for the arm to receive commands from the controller. Data logging happened in 30 s intervals where all recorded values were compared and averaged out to find the time delay of the device. The FCU had 200 data points and the time delay in all points was plotted (see Section 3.1).

To measure the operating speed of the arm's ESP32 microcontroller when in use, a code was implemented into the arm's control code to log the time delay for each subsystem. Excel Data Streamer was then used to record each trigger that was set in place by this new code. The triggers were sent to Excel, and the time was taken when each trigger was noticed. A start trigger was activated when the device received the transmission from the FCU, and an end trigger was activated once the device finished its current action. For example, if the FCU sent a command to close the fingers by one step, the start trigger would be activated as soon as the message was received, and the end trigger would be activated when the device finishes moving the fingers by one step. Using this method, the time delay

for each wrist pronation/supination, wrist flexion/extension, and finger movement was logged and plotted (see Section 3.1).

To measure the gripping force of the proof-of-concept Persistence hand, a BASELINE digital hand dynamometer (Model: 12-0070, capacity: 136 kg, resolution: 0.045 kg, accuracy: 1% of full scale), shown in Figure 16a, was used. The hand was put in the power grip pose and wrapped around the dynamometer to determine the grip strength.

(**a**) (**b**)

Figure 16. (**a**) Grip force test, (**b**) Pulling force test.

To measure the pulling strength of the arm, an exercise handle was attached to a digital scale (Brand and model: Dr. Meter ES-PS01 (Manufacturer: Dr. Meter, Newark, CA, USA), capacity: 50 kg, resolution: 0.010 kg), and the arm was pulled to measure the maximum pulling force, as shown in Figure 16b.

3. Results

3.1. Wireless Transmission Speed Tests

Figure 17 shows the time delay of all data points in the wireless transmission speed test. The "transmissions" in the abscissa refers to the total number of acknowledged messages or data packets successfully sent from one device to another. In this context, "acknowledged" indicates that the receiving device has confirmed receipt of the message, ensuring reliable communication between devices. This metric helps keep track of successful data exchanges and evaluates the efficiency of the communication system. The average transmission delay was 43.4 ms. Using Bluetooth and WiFi wireless transmission protocols proved that these devices are fast enough to get an almost instant response time for the user.

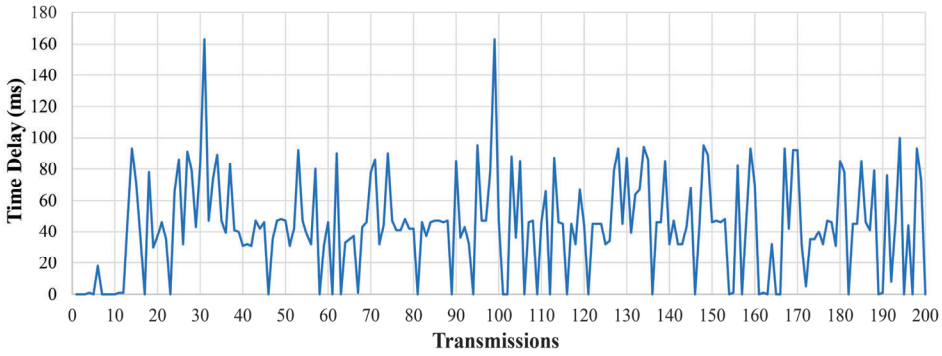

Figure 17. Time delay in wireless transmission of data from the FCU to the prosthetic arm.

The delay in response time of wrist pronation/supination, wrist flexion/extension, and finger movement are shown in Figures 18–20, respectively. Wrist pronation and supination

(Figure 18), had average delays of 160.8 µs and 157.0 µs, respectively. Wrist flexion and extension (Figure 19), had average delays of 141.8 and 149.4 µs, respectively. Any finger movement (Figure 20) has a delay of 280.5 µs. These time delays are very short and prove that the arm's microprocessor can handle the current subsystems at adequate speeds.

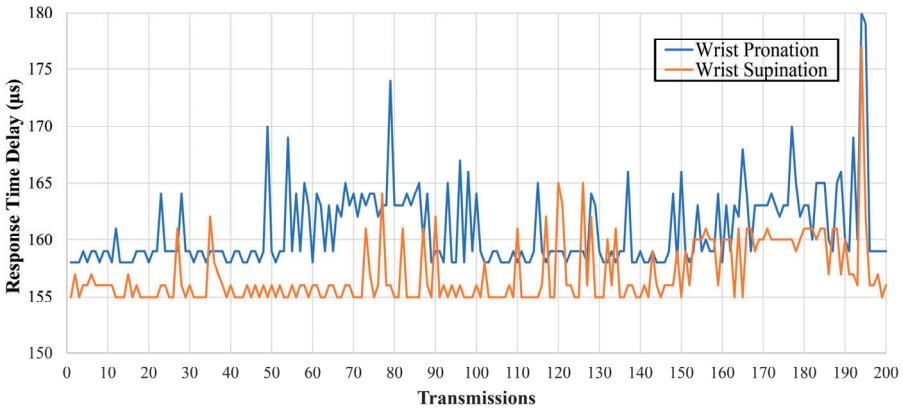

Figure 18. Response time delay in wrist pronation/supination data.

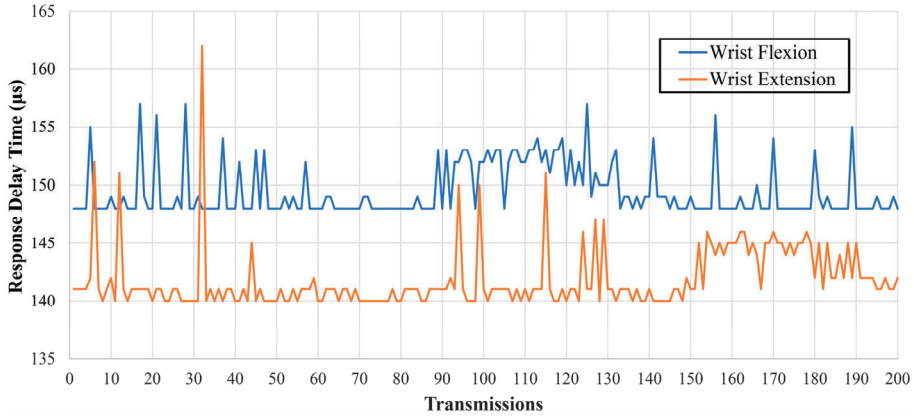

Figure 19. Response time delay in wrist flexion/extension data.

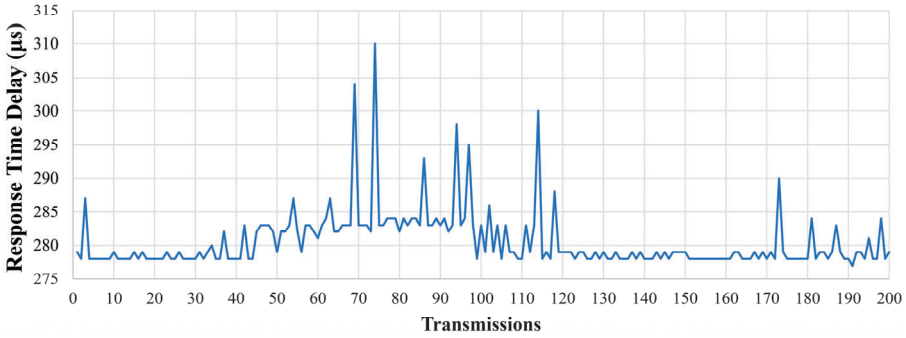

Figure 20. Response time delay in finger actuation data.

3.2. Gripping Tests

The prosthetic arm can possibly perform different grips and gestures that the user desires, but it comes pre-programmed with the five starting poses shown in Figure 21. The user can cycle through the available poses using the FCS by pressing on both push buttons at the same time.

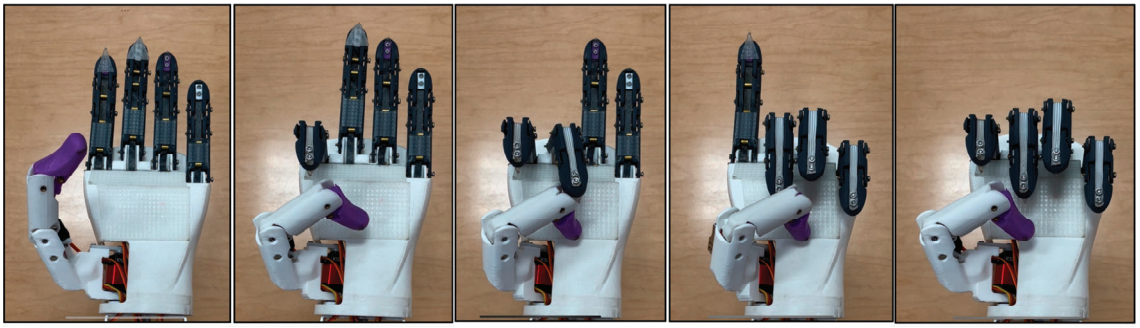

Figure 21. Default grips and gestures in Persistence Arm: Relaxed, pinch, tripod, point, and power.

To have a precise hand orientation adjustment around the object to be gripped, the wrist actuation system enables wrist flexion/extension and pronation/supination in response to the ankle inversion/eversion and dorsiflexion/plantarflexion motions, as demonstrated in Figure 22. In addition, the partial actuation capability allows for more precise control over the wrist orientation and finger actuation to take into consideration the shape and fragility of the object being held. Figure 23 illustrates this feature using wrist supination and power grip as examples.

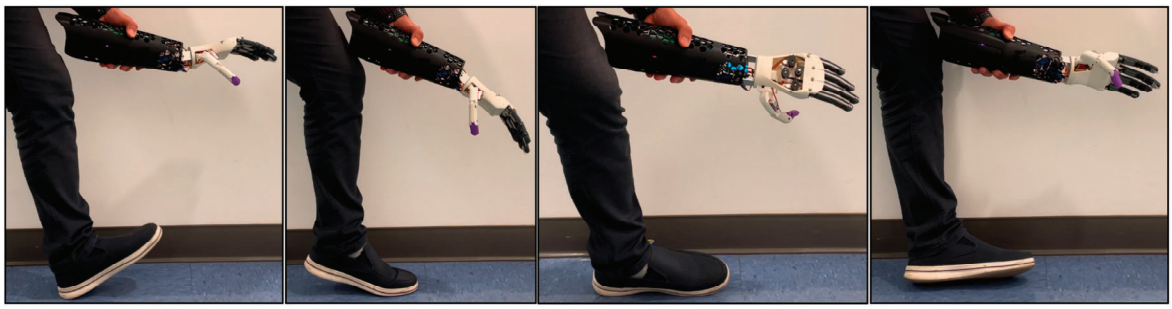

Figure 22. Wrist flexion/extension and pronation/supination.

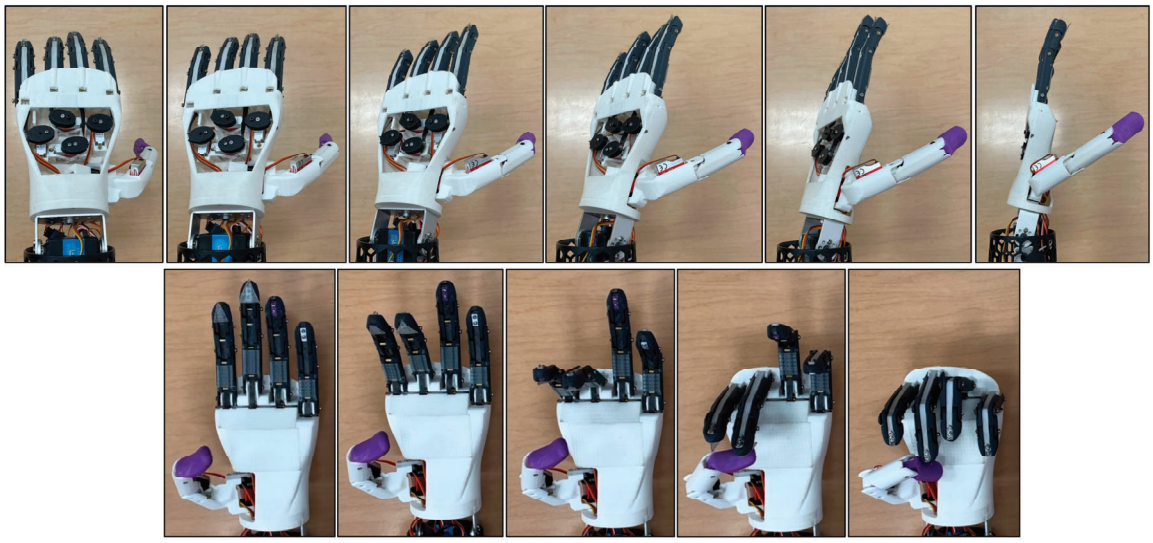

Figure 23. Partial actuation demonstration in wrist supination (**top**) and power grip (**bottom**).

Applying a grip force on the dynamometer has different dynamics than gripping regular household objects because the device requires applying force in one specific direction

to measure the force. Despite this challenging requirement, the maximum grip force of the prosthetic arm was found to be 2.8 kg (Figure 16a).

The pull strength test (Figure 16b) showed that the prosthetic fingers started to lose grip at 12.7 kg, giving the prosthesis a maximum vertical holding weight of 12.7 kg. A similar test was performed with just the wrist. In this test, the wrist showed a maximum holding weight of 40.8 kg before the servomotors started to show mechanical failure. In all the tests performed above, mechanical failure of the servomotors was experienced before structural failure of the 3D-printed parts in the arm.

Figure 24 shows Persistence arm gripping different household objects of different shapes, weights, and sizes using power, tripod, and pinch grips. The gripped objects include a hand tool, a Dremel tool, tape rolls of different sizes, plastic cups, empty and full bottles, a screwdriver, an apple, a rubber ball, a wireless computer mouse, a pencil, a small superglue bottle, a USB flash drive, and various 3D-printed objects. Video S1 shows the Persistence arm in action gripping various objects.

Figure 24. Persistence arm gripping different objects of various shapes, weights, and sizes.

4. Discussion

The Persistence arm has a lot of attractive features. The fact that most structural components are 3D-printed makes it easy for users to replace any part or change the color

or material of any component. The flexible carbon-fiber tendons led to a relatively higher grip strength from the fingers. The thumb has two degrees of freedom, leading to a more dexterous gripping capability. The response time delay in actuating all servomotors is very low, as shown in Figures 18–20. However, like any other prosthetic arm design, Persistence arm has some limitations. The arm is suitable for performing daily tasks like gripping various household items and showing specific gestures. The arm is not meant to be used for athletic activities or for carrying heavy weights. The arm is not waterproof, so it cannot operate underwater. A flexible covering of the arm, like the one used on LUKE arm (https://mobiusbionics.com/luke-arm/, accessed on 17 February 2025), is a possible design extension. The arm is also not meant to be used at elevated temperatures. The maximum service temperature of PLA material is around 50 °C, beyond which the PLA components might start to deform. This service temperature can be increased if another material with higher thermal resistance, such as ABS, is used for all parts. The Persistence arm has two wrist degrees of freedom, which are flexion/extension and pronation/supination. However, the radial/ulnar deviation degree of freedom was not considered given its relative low importance compared to the other two wrist degrees of freedom. For users with a long residual limb below the elbow, the whole forearm can be replaced by a shorter version that only includes the essential electronic components, without the wrist actuation mechanism to accommodate for the long residual limb.

Like any other electronic device, the batteries in the arm and the foot controller need to be charged. The estimated approximate operation time with a single full charge of each battery can be estimated as battery capacity (Ah)/current draw (A). For the arm, each finger servomotor draws 0.2 A, except the thumb abduction/adduction KST A12-610 servomotor that draws 1.2 A. Each of the two wrist servomotors draws 2.3 A. This current draw happens when the servomotors are applying the maximum torque they can apply. The arm's 7.4 V LiPo battery has a maximum charge of 5 Ah. If all hand servomotors are actuated to apply the maximum force, while the wrist servomotors are not experiencing any load, the estimated battery life would be 2.27 h (136 min) of constant maximum grip force. In the rare situation that all wrist and hand servomotors are applying their maximum force continuously, the estimated battery life would go down to 0.74 h (44 min). If the servomotors are not continuously experiencing force on them to apply their maximum torque, the current draw would be much smaller, leading to much higher battery life (8–12 h). As for the foot controller, the device draws a maximum current of 20 mA when in use and transmitting. When not in use, the current draw is only 9 mA. The battery capacity of the foot controller is 400 mAh. Hence, when in continuous use, the battery life would be 20 h, and when idle, the battery life would be 44 h, approximately. Although for many users a full charge of each battery would be enough for a single day usage, having a second battery for the arm and the foot controller would ensure that the user can spend a long day with continuous usage of the arm. Replacing the batteries is a simple task that would take a single-handed adult only a few minutes to be done.

Persistence arm's finger design includes three joints per finger actuated with one servomotor, so it is an underactuated mechanism. This gives it the compliance feature, enabling the hand to be adaptive to the shape of the object being gripped. Eliminating the distal interphalangeal (DIP) joint, and replacing the distal and middle phalanges with one pre-deformed distal-middle phalange, like the one used in Infinity arm's fingers [15], would lead to a stiffer finger design.

A recent review paper by Siegel et al. [37] showed that there is a lack of standardization in upper-limb prostheses testing, and that developers often use custom, study-specific tests to validate their novel devices. Clinical settings and research laboratories differ in their time constraints, access to specialized equipment, and testing objectives. Testing of the proposed

system was done to assess the performance of the manufactured prototypes focusing on specific engineering aspects. Further tests will be performed in the future, focusing on the standard outcome measures [38], such as the Box and Block (BB) test, University of New Brunswick (UNB) skill and spontaneity tests, Activities Measure for Upper Limb Amputation (AM-ULA) test, Upper Extremity Functional Scale (UEFS) tests, and the Patient-Specific Functional Scale (PSFS) tests, following the works of Resnik et al. [39–41].

The Infinity-2 foot controller also came with new features, compared to the first design reported in [15]. The speed of wireless transmission is extremely high as was shown in Figure 17, thanks to the Bluetooth and Wi-Fi technology enabled in the used microcontroller. The controller can be worn comfortably inside a shoe, on a sock, or barefoot. The controller enables using the toes to fully control the prosthetic arm fingers and simple ankle motions to control wrist actuation. Unlike many other previously documented prostheses' control systems, the proposed controller allows for gradual finger actuation rather than an on/off arrangement. Gradual control of fingers and wrist servomotors enable the user to orient the hand properly around the object being gripped and adjust the grip force precisely to match the weight and structure of the object. This would prevent crushing fragile objects or slippage of smooth or heavy objects. It is known that myoelectric prosthetic hand users have difficulty with, and frequently avoid, grasping fragile objects with their prosthesis [42]. This required Fishel et al. [42] to develop a contact detection reflex system that was integrated into a commercial myoelectric prosthetic hand to adjust the gripping force automatically upon contacting fragile objects. However, such a solution is still depriving the user of fully controlling the grip of the arm. Users might still want to be capable of applying larger gripping forces on some objects than what a reflex system would allow, i.e., to reshape a deformable item or to intentionally crush a plastic cup. Only a system that gives the user full control over the applied gripping force, like the proposed system, could enable that. The controller also offers cycling between different grips and gestures. Preliminary testing done by the developers showed that learning how to use such a controller is significantly easy, requiring a natural toe dexterity. With 15–30 min of practice in the first use, users can be proficient in using the controller. Previous foot controller developers, such as Carrozza et al. [26,27], have also reported ease of adaptation and learning. The controller is independent of the presence of muscles in the residual limb.

Preliminary tests showed that some individuals can significantly increase the chances of success in pressing on the buttons if they raise the big toe slightly up when pressing with the lesser toes and raise the lesser toes slightly up when pressing with the big toe, as shown in Figure 25a. Other individuals preferred to slightly turn the whole foot (inversion or eversion) to press on the left or the right panel, as shown in Figure 25b. Only these simple toe articulations are needed to have full control over the gradual finger deformation.

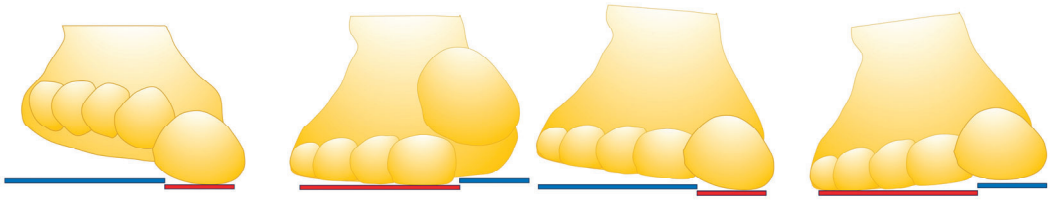

(**a**) (**b**)

Figure 25. Toe articulations needed to perform finger opening and closing actuations: (**a**) option 1, (**b**) option 2.

This controller, however, still has some limitations. First, the user should have at least one functioning foot with the ability to move the ankle and the toes (ankle and toe mobility).

Being waterproof was not one of the main goals of the current iteration. However, sealing the FCU and the electronics on the FCS will be a future design extension. The controller has a walking detection system that would freeze the arm during walking. So, the controller can be used only while standing or sitting. A dual control approach can be developed to enable voice control, for example, to control the arm while walking, if there is a need for such a capability. A similar dual control was presented in [9,10]. The code of the proposed foot controller can be easily adjusted to control other prosthetic arms on the market if communication protocols are established between the arm and the controller.

5. Conclusions

Controlling prosthetic arms with foot controllers could be a promising alternative control method to EMG controllers that have a lot of drawbacks, resulting in a high abundance rates of upper limb prostheses. The Infinity-2 foot controller proposed in this work can be used even barefoot because of the new sleeve design that secures the controller around the forefoot. The wireless transmission between the foot controller and the prosthetic arm happens in a fraction of a second, giving almost an immediate effect. The controller can fully control a five-finger prosthetic arm equipped with a two-degree-of-freedom wrist actuation system. It offers gradual control of the fingers to adjust the gripping force based on the fragility, texture, and weight of the object to be gripped. Various grips and gestures that actuate specific groups of fingers can also be performed. Preliminary tests by the developers showed that the system is intuitive, and that training time needed to use the system comfortably is short for most individuals, making it an attractive prosthetic arm control method that does not rely on any remaining muscles in the residual limb. It could also be used by individuals who put on temporary casts after breaking their wrists.

The Persistence arm is a new addition to the transradial 3D-printed prosthetic arm designs that can be used to perform average household daily tasks. It features a two-degree-of-freedom wrist actuation mechanism, and a hand with five fingers individually actuated. The three-phalange underactuated forefinger design and the two-degree-of-freedom linkage-based thumb gave the hand an adaptive performance similar to that of a human hand. Preliminary testing in the current study proved the effectiveness of the proposed designs, offering new alternatives to prosthetic arm users for higher quality of life beyond the trauma of missing the functionality of the human arm.

6. Patents

Utility Patent Application Number: 18/648726, Filing date: 4/29/2024. Title: "Foot Controller for Prosthetic Arms, Their Methods of Production and Use" (Inventors: Peter L. Bishay and Jack Wilgus).

Supplementary Materials: The following supporting information can be downloaded at: https://www.mdpi.com/article/10.3390/technologies13030098/s1, Video S1: Persistence Arm with Infinity-2 Foot Controller System.

Author Contributions: Conceptualization, P.L.B.; methodology, all authors; software, all authors; validation, P.L.B., G.F.A. and I.S.; formal analysis, P.L.B., G.F.A. and I.S.; investigation, all authors; resources, P.L.B.; data curation, P.L.B., G.F.A. and I.S.; writing—original draft preparation, P.L.B., G.F.A. and I.S.; writing—review and editing, P.L.B.; visualization, P.L.B., G.F.A. and I.S.; supervision, P.L.B.; project administration, P.L.B., G.F.A. and I.S.; funding acquisition, P.L.B. All authors have read and agreed to the published version of the manuscript.

Funding: This research received no external funding.

Institutional Review Board Statement: Ethical review and approval were waived by the CSUN IRB for this study since the preliminary testing was determined not to be human subjects research.

No human subjects outside the research team were involved in the preliminary testing of the proposed system.

Informed Consent Statement: Not Applicable.

Data Availability Statement: The data presented in this study is available on request from the corresponding author.

Acknowledgments: This work was performed by the seventh cohort of the "Smart Prosthetics" research-based senior design project at California State University, Northridge (CSUN). The authors acknowledge the Mechanical Engineering Department, the Instructionally Related Activities (IRA) grant, and the Student Travel and Academic Research (STAR) program at CSUN.

Conflicts of Interest: The authors declare no conflicts of interest.

Appendix A

The wiring diagram of the foot controller sleeve and unit is shown in Figure A1, whereas the Persistence arm's wiring diagram is shown in Figure A2.

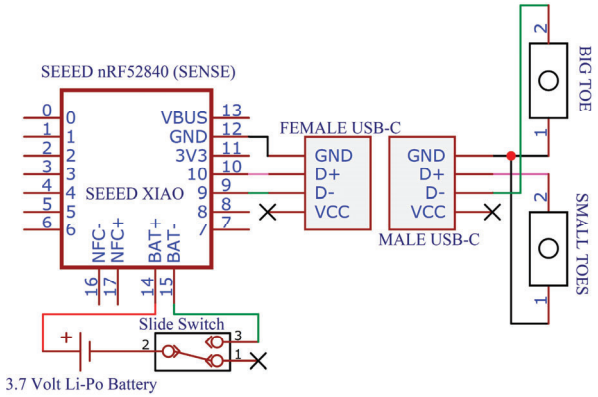

Figure A1. Wiring diagram for FCU and FCS.

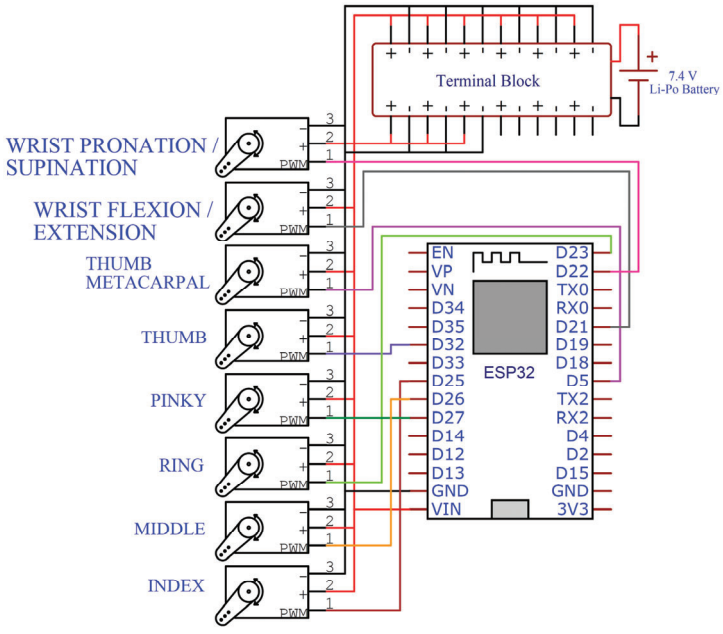

Figure A2. Wiring diagram for Persistence Arm.

Appendix B

The starting shape of the wrist servo mount, shown in Figure A3a, was used in the generative design study. This geometry was reduced to better represent the load conditions. Using a starting shape was an optional step, taken to reduce the number of iterations. Since the main goal of the part was to provide a good mount for the pan-tilt wrist actuation system, the reduced shape was then used to divide the part into different regions. These regions are divided into two categories: preserve regions, where the GD part would connect to the shell of the arm (shown in green in Figure A3b), and obstacle regions, which leave room for both the servo motor to connect and wires to be run through (shown in red in the figure). The load conditions featured an axial load of 180 N in the respective −Z direction distributed among the top screw holes and another 180 N in the respective +Z direction. It also featured a 30 N load upon the side connection to the shell in the respective +Y direction, as well as a mirrored 30 N load upon the other side connection. These values simulated a scenario in which the arm was oriented perpendicular to the ground, and holding 180 N weight. To better represent the strength of the material, the study utilized a custom material profile of Bambu ABS filament with 15% gyroid infill. The profile used tensile strength, yield strength, density, and Young's modulus values that were experimentally determined utilizing a modified ASTM D638 test. The manufacturing method was set to additive manufacturing in the +Z direction and with an overhang angle of 45°. Finally, the goal of the study was set to minimize mass, and a minimum factor of safety of 3.0 was specified. The generated design is shown in Figure A3c. The part was then printed on a Bambu P1P printer with the same settings as the ASTM D638 test coupons.

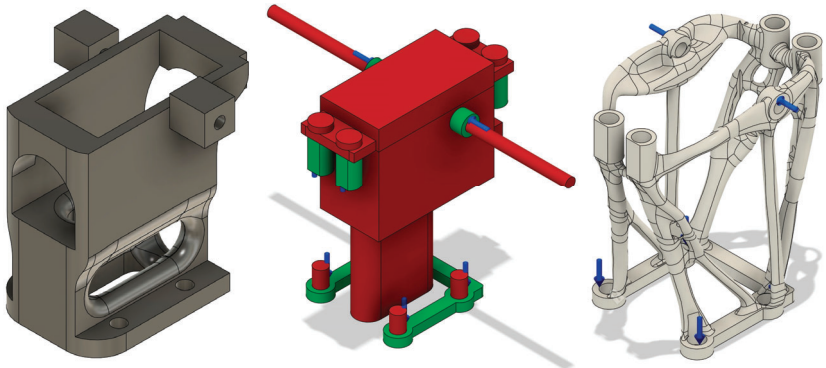

(**a**) (**b**) (**c**)

Figure A3. (**a**) Starting shape of the wrist servo mount with reduced geometry, (**b**) GD model with preserve (green) and obstacle (red) regions, (**c**) Generated design of the mount.

References

1. Salminger, S.; Stino, H.; Pichler, L.H.; Gstoettner, C.; Sturma, A.; Mayer, J.A.; Szivak, M.; Aszmann, O.C. Current rates of prosthetic usage in upper-limb amputees—Have innovations had an impact on device acceptance? *Disabil. Rehabil.* **2022**, *44*, 3708–3713. [CrossRef] [PubMed]
2. Biddiss, E.A.; Chau, T.T. Upper limb prosthesis use and abandonment: A survey of the last 25 years. *Prosthet. Orthot. Int.* **2007**, *31*, 236–257. [CrossRef] [PubMed]
3. Chen, Z.; Min, H.; Wang, D.; Xia, Z.; Sun, F.; Fang, B. A Review of Myoelectric Control for Prosthetic Hand Manipulation. *Biomimetics* **2023**, *8*, 328. [CrossRef] [PubMed]
4. Chadwell, A.; Kenney, L.; Thies, S.; Head, J.; Galpin, A.; Baker, R. Addressing unpredictability may be the key to improving performance with current clinically prescribed myoelectric prostheses. *Sci. Rep.* **2021**, *11*, 3300. [CrossRef]
5. Franzke, A.W.; Kristoffersen, M.B.; Bongers, R.M.; Murgia, A.; Pobatschnig, B.; Unglaube, F.; van der Sluis, C.K. Users' and therapists' perceptions of myoelectric multi-function upper limb prostheses with conventional and pattern recognition control. *PLoS ONE* **2019**, *14*, e0220899. [CrossRef]

6. Vujaklija, I.; Farina, D.; Aszmann, O.C. New developments in prosthetic arm systems. *Orthop. Res. Rev.* **2016**, *8*, 31–39. [CrossRef]
7. Bandara, D.; Arata, J.; Kiguchi, K. Towards Control of a Transhumeral Prosthesis with EEG Signals. *Bioengineering* **2018**, *5*, 26. [CrossRef]
8. Vilela, M.; Hochberg, L.R. Applications of Rain-computer interfaces to the control of robotic and prosthetic arms. In *Handbook of Clinical Neurology*; Elsevier: Amsterdam, The Netherlands, 2020; pp. 87–99. [CrossRef]
9. Bishay, P.L.; Fontana, J.; Raquipiso, B.; Rodriguez, J.; Borreta, M.J.; Enos, B.; Gay, T.; Mauricio, K. Development of a biomimetic transradial prosthetic arm with shape memory alloy muscle wires. *Eng. Res. Express* **2020**, *2*, 035041. [CrossRef]
10. Bishay, P.; Aguilar, C.; Amirbekyan, A.; Vartanian, K.; Arjon-Ramirez, M.; Pucio, D. Design of a Lightweight Shape Memory Alloy Stroke-Amplification and Locking System in a Transradial Prosthetic Arm. In Proceedings of the ASME 2021 Conference on Smart Materials, Adaptive Structures and Intelligent Systems, Virtual, 14–15 September 2021; American Society of Mechanical Engineers: New York, NY, USA, 2021; p. V001T05A015.
11. Arias, L.M.; Iwaniec, M.; Pirowska, P.; Smoleń, M.; Augustyniak, P. Head and Voice-Controlled Human-Machine Interface System for Transhumeral Prosthesis. *Electronics* **2023**, *12*, 4770. [CrossRef]
12. Ozsahin, D.U.; Duwa, B.B.; Idoko, J.B.; Edward, D.; Khorzom, L.; Hussein, O.H.; Alsiba, A.; Hamzah, N.; Ozsahin, I. Voice-controlled prosthetic hand. In *Practical Design and Applications of Medical Devices*; Elsevier: Amsterdam, The Netherlands, 2024; pp. 99–106. [CrossRef]
13. Yang, H.; Tao, Z.; Yang, J.; Ma, W.; Zhang, H.; Xu, M.; Wu, M.; Sun, S.; Jin, H.; Li, W.; et al. A lightweight prosthetic hand with 19-DOF dexterity and human-level functions. *Nat. Commun.* **2025**, *16*, 955. [CrossRef]
14. Resnik, L.; Klinger, S.L.; Etter, K. The DEKA Arm: Its features, functionality, and evolution during the Veterans Af-fairs Study to optimize the DEKA Arm. *Prosthet. Orthot. Int.* **2014**, *38*, 492–504. [CrossRef] [PubMed]
15. Bishay, P.L.; Wilgus, J.; Chen, R.; Valenzuela, D.; Medina, V.; Tan, C.; Ittner, T.; Caldera, M.; Rubalcava, C.; Safarian, S.; et al. Controlling a Below-the-Elbow Prosthetic Arm Using the Infinity Foot Controller. *Prosthesis* **2023**, *5*, 1206–1231. [CrossRef]
16. Lyons, K.R.; Joshi, S.S. A Case Study on Classification of FOOT Gestures Via Surface Electromyography. In Proceedings of the Annual Rehabilitation Engineering and Assistive Technology Society of North America Conference, Denver, CO, USA, 10–14 June 2015; pp. 1–5.
17. Lyons, K.R.; Joshi, S.S. Real-time evaluation of a myoelectric control method for high-level upper limb amputees based on homologous leg movements. In Proceedings of the 2016 38th Annual International Conference of the IEEE Engineering in Medicine and Biology Society (EMBC), Orlando, FL, USA, 6–20 August 2016; pp. 6365–6368.
18. Lyons, K.R.; Joshi, S.S. Upper Limb Prosthesis Control for High-Level Amputees via Myoelectric Recognition of Leg Gestures. *IEEE Trans. Neural Syst. Rehabil. Eng.* **2018**, *26*, 1056–1066. [CrossRef] [PubMed]
19. Resnik, L.; Klinger, S.L.; Etter, K.; Fantini, C. Controlling a multi-degree of freedom upper limb prosthesis using foot controls: User experience. *Disabil. Rehabil. Assist. Technol.* **2014**, *9*, 318–329. [CrossRef] [PubMed]
20. Lee, S.; Sung, M.; Choi, Y. Wearable fabric sensor for controlling myoelectric hand prosthesis via classification of foot postures. *Smart Mater. Struct.* **2020**, *29*, 035004. [CrossRef]
21. Marinelli, A.; Boccardo, N.; Tessari, F.; Di Domenico, D.; Caserta, G.; Canepa, M.; Gini, G.; Barresi, G.; Laffranchi, M.; De Michieli, L.; et al. Active upper limb prostheses: A review on current state and upcoming breakthroughs. *Prog. Biomed. Eng.* **2023**, *5*, 012001. [CrossRef]
22. Alderson, S.W. Electrically Operated Artificial Arm for Above-The-Elbow Amputees. U.S. Patent US2580987A, 1 January 1952.
23. Klopsteg, P.E.; Wilson, P.D. *Human Limbs and Their Substitutes: Presenting Results of Engineering and Medical Studies of the Human Extremities and Application of the Data to the Design and Fitting of Artificial Limbs and to the Care and Training of Amputees*; Hafner: Cleveland, OH, USA, 1968.
24. Graupe, D. Control of upper-limb prostheses in several degrees of freedom. *Bull. Prosthet. Res.* **1974**, *22*, 226–236.
25. Luzzio, C.C. Controlling an Artificial Arm with Foot Movements. *Neurorehabilit. Neural Repair* **2000**, *14*, 207–212. [CrossRef]
26. Carrozza, M.; Persichetti, A.; Laschi, C.; Vecchi, F.; Lazzarini, R.; Tamburrelli, V.; Vacalebri, P.; Dario, P. A Novel Wearable Interface for Robotic Hand Prostheses. In Proceedings of the 9th International Conference on Rehabilitation Robotics, ICORR 2005, Chicago, IL, USA, 28 June–1 July 2005; pp. 109–112.
27. Carrozza, M.C.; Persichetti, A.; Laschi, C.; Vecchi, F.; Lazzarini, R.; Vacalebri, P.; Dario, P. A Wearable Biomechatronic Interface for Controlling Robots with Voluntary Foot Movements. *IEEE/ASME Trans. Mechatron.* **2007**, *12*, 1–11. [CrossRef]
28. Innovations. DEKA, (n.d.). Available online: https://dekaresearch.com/innovations/ (accessed on 28 January 2025).
29. Lanier, G.R., Jr.; Perry, N.C.; Pascoe, A.P.; Van der Merwe, D.A. Method and apparatus for control of a prosthetic. U.S. Patent US20220117759A1, 21 April 2022.
30. Lanier, G.R., Jr.; Perry, N.C.; Pascoe, A.P.; Van der Merwe, D.A. Apparatus for control of a prosthetic. U.S. Patent US9901465B2, 27 February 2018.
31. The Hero Arm Overview is a Prosthetic Arm Made by Open Bionics, (n.d.). Available online: https://openbionics.com/hero-arm-overview/ (accessed on 26 January 2025).

32. Piazza, C.; Grioli, G.; Catalano, M.; Bicchi, A. A Century of Robotic Hands. *Annu. Rev. Control. Robot. Auton. Syst.* **2019**, *2*, 1–32. [CrossRef]
33. Michelangelo Hand | The Michelangelo Hand Helps You Regain Extensive Freedom, (n.d.). Available online: https://www.ottobock.com/en-us/product/8E500 (accessed on 26 January 2025).
34. i-Limb® Quantum Bionic Hand. Ossur.com, (n.d.). Available online: https://www.ossur.com/en-us/prosthetics/arms/i-limb-quantum (accessed on 26 January 2025).
35. bebionic Hand | The Most Lifelike Prosthetic Hand, (n.d.). Available online: https://www.ottobock.com/en-us/product/8E7* (accessed on 26 January 2025).
36. Wendo, K.; Barbier, O.; Bollen, X.; Schubert, T.; Lejeune, T.; Raucent, B.; Olszewski, R. Open-Source 3D Printing in the Prosthetic Field—The Case of Upper Limb Prostheses: A Review. *Machines* **2022**, *10*, 413. [CrossRef]
37. Siegel, J.R.; Battraw, M.A.; Winslow, E.J.; James, M.A.; Joiner, W.M.; Schofield, J.S. Review and critique of current testing protocols for upper-limb prostheses: A call for standardization amidst rapid technological advancements. *Front. Robot. AI* **2023**, *10*, 1292632. [CrossRef]
38. Miller, L.A.P.; Swanson, S.O. Introduction to the Academy's State of the Science Conference on Upper Limb Prosthetic Outcome Measures. *JPO J. Prosthet. Orthot.* **2009**, *21*, 1–2. [CrossRef]
39. Resnik, L.; Borgia, M. Reliability and Validity of Outcome Measures for Upper Limb Amputation. *JPO J. Prosthet. Orthot.* **2012**, *24*, 192–201. [CrossRef]
40. Resnik, L.; Adams, L.; Borgia, M.; Delikat, J.; Disla, R.; Ebner, C.; Walters, L.S. Development and Evaluation of the Activities Measure for Upper Limb Amputees. *Arch. Phys. Med. Rehabil.* **2013**, *94*, 488–494.e4. [CrossRef]
41. Resnik, L.; Borgia, M. Responsiveness of outcome measures for upper limb prosthetic rehabilitation. *Prosthet. Orthot. Int.* **2016**, *40*, 96–108. [CrossRef]
42. Fishel, J.A.; Matulevich, B.; Muller, K.A.; Berke, G.M. The (Sensorized) Hand is Quicker than the Eye: Restoring Grasping Speed and Confidence for Amputees with Tactile Reflexes. In Proceedings of the 2019 International Conference on Robotics and Automation (ICRA), Montreal, QC, Canada, 20–24 May 2019; pp. 5097–5102.